NATIONAL ADVISORY COMMITTEE FOR AERONAUTICS

TECHNICAL NOTE

No. 1432

CHANGES FOUND ON RUN-IN AND SCUFFED SURFACES OF STEEL, CHROME PLATE, AND CAST IRON

By J. N. Good and Douglas Godfrey

Flight Propulsion Research Laboratory
Cleveland, Ohio

Washington
October 1947

NATIONAL ADVISORY COMMITTEE FOR AERONAUTICS

TECHNICAL NOTE NO. 1432

CHANGES FOUND ON RUN-IN AND SCUFFED SURFACES OF STEEL, CHROME PLATE, AND CAST IRON

By J. N. Good and Douglas Godfrey

SUMMARY

A study was made of run-in and scuffed steel, chrome-plate, and cast-iron surfaces. X-ray and electron diffraction techniques, microhardness determinations, and microscopy were used. Surface changes varied and were found to include three classes: chemical reaction, hardening, and crystallite-size alteration. The principal chemical reactions were oxidation and carburization with the following reaction products:

Specimen	Surface condition	Material identified on surface	Questionable identification[1]
SAE 4140 steel reciprocating slider	Unrun	α-Fe	Fe_3O_4
	Worn unscuffed	α-Fe	Fe_3O_4, Fe_2O_3
	Scuff recovered	α-Fe, Fe_3O_4	Fe_3C, Fe_2O_3
	Scuffed	α-Fe, Fe_3C, Fe_3O_4	Fe_2O_3
SAE 4140 steel aircraft-engine cylinder barrel	Worn unscuffed (Superficial face)	C (graphite), Beilby layer	Mixed oxides
	(Less than 0.001 in. below surface face)	α-Fe, Fe_3O_4, Fe_2O_3	- - - - - - - -
Chrome-plated cast-iron rider	Worn unscuffed	α-Cr	- - - - - - - -
	Burnished	α-Cr, Cr_2O_3, Cr_3C_2	- - - - - - - -
	Scuffed	α-Cr, Cr_2O_3, Cr_3C_2	- - - - - - - -
Cast-iron reciprocating slider	Unrun	α-Fe	Fe_3C
	Worn	α-Fe	C (graphite)
	Scuffed	α-Fe	C (graphite)

[1]Lines best fit pattern of material listed.

Hardness of materials examined varied with degree of surface condition. The crystallite sizes were in the order of 10^{-7} centimeters. The sizes changed with condition of operation.

INTRODUCTION

The changes that occur to rubbing metallic surfaces have been studied by many investigators in order to obtain a better understanding of the phenomena of wear and wear resistance. (See the bibliography.) A study of the bibliography and the reference reports reveals that at least the following factors are of importance:

1. Formation of surface films and reaction products
2. Changes in surface hardness
3. Changes in crystallite size

Some relations are established herein among these factors and the phenomena of run-in and one phase of wear, scuffing, by identification of and examination of surface changes occurring with one of the well-known sources of metallic wear, reciprocating sliding. The term "run-in" is used in this report to designate the process through which surfaces acquire, by mutual interaction during sliding contact, increased capacity to carry load and to withstand wear. This investigation neglects the relation of hydrodynamic and boundary lubrication to run-in, although all surfaces studied were lubricated.

Changes in the surface composition and surface characteristics were studied under run-in and wear conditions for steel (SAE 4140) rubbed against cast iron, chrome-plated cast iron rubbed against steel, and cast iron rubbed against cast iron; these combinations are standard in aircraft engines. Use was made in this investigation of specialized techniques in X-ray and electron diffraction, of chemical and metallographic analyses, and of hardness measurements.

APPARATUS AND PROCEDURE

Specimens of standard aircraft-engine cylinder-barrel and piston-ring material combinations used in these examinations were obtained from two sources. Portions of used cylinder barrels and piston rings were directly examined, whereas portions of unused cylinder barrels and piston rings were examined after rubbing under pressure in a reciprocating slider machine. Surface changes on the specimens were examined by

X-ray and electron diffraction. Supplementary information was obtained by chemical and microchemical analysis, electrographic analysis, metallographic examination, and microhardness determination.

The following materials were investigated:

Material combination	Specimen examined	Specimen source
SAE 4140 steel slider rubbed against cast-iron rider	Slider	Slider machine
Cast-iron piston rings rubbed against SAE 4140 steel cylinder barrel	Cylinder barrel	Aircraft engine
SAE 4140 steel slider rubbed against chrome-plated cast-iron rider	Rider	Slider machine
Cast-iron slider rubbed against cast-iron rider	Slider	Slider machine
Chrome-plated cast-iron piston rings rubbed against SAE 4140 steel cylinder barrel	Ring	Aircraft engine

This selection of specimens is representative of the materials used in standard aircraft engines and should give results representative of run-in and scuff in those engines.

The slider machine (fig. 1) reciprocated a slider specimen $7\frac{1}{2}$ by $1\frac{1}{2}$ inches beneath a fixed and loaded rider $1\frac{1}{8}$ by $\frac{1}{8}$ inches. The rider was loaded by applied gas pressure, which was read from a dial. Mass temperatures of the rider and the slider were recorded with thermocouples. When the surfaces are lubricated, as in this investigation, conditions of both boundary and hydrodynamic lubrication are believed to exist, that of boundary at the ends of the stroke and that of hydrodynamic at the middle of the stroke. The oil used was Navy 1120 fed at a rate of 16 cubic centimeters per hour. The reciprocating speed was 630 cycles per minute with a stroke of $5\frac{1}{2}$ inches. The procedure used for all specimens was as follows:

1. The two mating surfaces were lapped with silicon carbide lapping compound with resultant surface-roughness readings of approximately 40 to 60 microinches rms for the rider and below 15 microinches rms for the slider.

2. The surfaces were cleaned with solvents.

3. The surfaces were mated by reciprocation under a constant load of 600 pounds per square inch applied to the rider for 15 minutes. Run-in began at this point.

4. For scuffed specimens, the rider was loaded in increments of 100 pounds per square inch every 5 minutes until scuffing occurred. A prolonged run-in procedure, consisting of operation at 2400 pounds per square inch for 2 hours followed by 100 pounds per square inch and temperature-stabilization increments until scuffing occurred, was used on one cast-iron surface. Scuffing observed visually, accompanied by rapid temperature rise, served as a criterion of surface failure. The machine was stopped within a few seconds after failure began, which was usually 2 to 3 hours after the start of the run.

The aircraft engines were operated for $5\frac{1}{2}$ to 7 hours of run-in plus 15 to 100 hours of endurance at an average engine speed of 2500 rpm and an average indicated mean effective pressure of 250 pounds per square inch.

All X-ray diffraction patterns were obtained with cobalt Kα radiation and with the specimen mounted in the manner used with the Debye-Scherrer powder camera. A 5-inch-diameter cylindrical camera was used with an iron-oxide filter. Diffraction-line intensities were visually estimated. A microphotometer could be used only to record α-iron X-ray-line position, breadth, and intensity for crystallite-size determination. Positive identification of compounds was made only when a minimum of three of the strongest lines was observed for each compound associated with at least one surface condition out of a series of surface conditions obtained for a given material. Calculations of crystallite size were made from line broadening according to the procedure given in reference 1 on the assumption that crystallite-size effects alone were causing line broadening. Fine copper powder was used to determine the standard line breadth. No estimation of the fraction of this broadening caused by lattice distortion was made. (Lattice distortion may have caused a great part of the broadening but no proved way exists to measure relative effects of lattice distortion and crystallite size.) If, in a group of lines composed of diffraction patterns of several compounds, one pattern obviously predominated in intensity, that compound was believed to be present in greater amounts than any of the others.

Electron diffraction examination of subsurface regions in the used engine specimens was made after each of five successive abrasions of the metal on 00 emery paper under pure benzene. The depth of an abrasion was measured with a vernier micrometer. Estimates of the depth of surface changes were made by microscopic measurements on cross and taper sections. Control specimens cut from the base structure of the engine cylinders were similarly treated and examined for evidence of any oxidation that might have been produced by abrasion.

Hardness measurements were made with either Knoop or Vickers indenters, depending upon the condition of the surface being investigated. The quantitative units thus obtained were checked qualitatively with a Bierbaum-scratch (Microcharacter) hardness tester. This scratch indentation is less affected by metallic strata underlying the surface than the other indenters, but it is more sensitive to surface irregularities.

Chemical and microchemical analyses were made on natural and metallographic surfaces by means of solution, electrographic, and electrolytic etches. Metallographic examinations were made on normal or on tapered and plating-reinforced cross sections.

RESULTS AND DISCUSSION

Steel Surfaces

With the slider-rider combination of SAE 4140 steel and cast iron, several conditions occurred successively in strips, or zones, on the steel slider (fig. 2). The production of more than one surface condition on one specimen was due to slightly imperfect mating of rider and slider. The manner in which surface changes progressed represents various steps in increased loading until failure. Identification of the surface conditions is as follows: A represents the original unworn (unrun) surface; B represents a worn but unscuffed surface; and C represents a surface that appeared to have entered an initial condition of scuff rather early in the experiment but to have almost immediately recovered. Close observation during the run revealed a momentary darkening in color and then a change to dark gray. The permanently scuffed surface that developed in several stages, which succeeded each other within a few seconds, is represented by D. The first stage of formation was indicated by the momentary appearance of a dark-brown or reddish-brown surface color, which changed to black. The change in color was accompanied by the appearance in the recovered oil of a sediment whose major constituent was analyzed as alpha ferric oxide α-Fe_2O_3 by X-ray diffraction methods.

The appearance of bright spots and heavy scuff marks on the surface accompanied by a sharp increase in temperature indicated permanent scuff. It appears that because of the initial imperfect mating a shifting of load took place, which led to variations and irregularities in local load concentrations. Surface B may be considered to have carried a large portion of the load during the mating procedure and therefore to have been able to support the load as it was increased. As the load was increased, surface C suddenly appeared. This appearance occurred as a result, possibly, of slight warping as the temperature rose and because surface C may have been insufficiently mated at the time the load increased. As the load was further increased, strip D appeared, possibly because of a combination of higher load and further warping until the surface scuffed rapidly with so much progressive damage that the scuff became extensive and permanent.

Identification of alpha iron, α-Fe, ferrosoferric (ferrosic) oxide, Fe_3O_4, and iron carbide, Fe_3C, in these surfaces was made by X-ray diffraction. (See fig. 3.) (Whenever Fe_3O_4 is mentioned herein, the possibility that it could also be γ-Fe_2O_3 should be considered, because the two are indistinguishable by usual diffraction methods.) On all four surfaces (A, B, C, and D), Fe_3O_4 was considered present and gave an apparent maximum diffraction intensity for scuff-recovered and a decreased intensity for scuffed conditions as judged from the number of lines and from the changes in visual intensity. The identification of Fe_2O_3 on surfaces B, C, and D was questionable. Iron carbide was identified on the scuffed surface D and questionably identified on scuff-recovered surface C. The intensities were greater for the scuffed than the scuff-recovered surface. No Fe_3C was identified on the unscuffed surfaces.

The results of the determination of crystalite sizes are presented in figure 4 and the X-ray patterns showing the differences are shown in figure 5. The hardness of the four surface conditions is also shown in figure 4; maximum hardness existed on the scuff-recovered surface.

Electron diffraction examination of specimens cut from an unscuffed SAE 4140 steel cylinder operated more than 100 hours with cast-iron rings and thoroughly cleaned with solvents on the outermost surface first produced the two diffuse halos characteristic of the Beilby layer and the diffraction pattern of graphite (fig. 3). Light abrasion with 00 emery, in successive steps under benzene, exposed metal that gave the diffraction patterns of α-Fe, Fe_3O_4, and Fe_2O_3. Oxides were thus detectable to depths estimated near 0.001 inch. Oxidation during the abrasion was proved negligible by the same treatment of control specimens.

This oxidation is shown in more detail in figure 6 and is labeled depth of oxygen penetration. Oxides existed beneath the surface of the metal everywhere the cylinder had been rubbed. The top 1/8 inch of the barrel was subjected to conditions within the combustion chamber but to no rubbing during engine operation because it was above the region of piston contact. In that top area the oxide existed only as a tenacious blue surface film under a carbon deposit. Variation in surface hardness is plotted on the same abscissa as the oxygen data in figure 6. These data were taken at five representative points along the barrel length.

Chrome Surfaces

The chrome-plated cast-iron rider that was reciprocated against the steel slider contained only three distinguishable surface conditions at the end of the run; namely, worn unscuffed, burnished, and normal scuff. Unrun-surface analyses were obtained from another rider.

The chrome pattern predominates in all the surface X-ray diffraction patterns. Diffraction examination showed no presence of any chromic oxide, Cr_2O_3, on the unscuffed surface although this surface was expected to contain at least a small amount of this oxide, possibly in the amorphous condition. The compounds Cr_2O_3 and chromium carbide, Cr_3C_2, were easily identified on the burnished and scuffed surfaces. An X-ray diffraction pattern containing evidence for these compounds on the scuffed surface is shown in figure 7. A number of diffraction lines that stand alone and belong to none of the previously mentioned compounds may be parts of the diffraction patterns of Fe_2O_3, Fe_3O_4, the chromium nitrides, Cr_2N and CrN, the chromium carbides, $Cr_{23}C_6$, Cr_7C_3, and also Fe_3C (on the scuffed surfaces). No completely reliable quantitative trends could be found because of some difficulty in rating diffraction intensities, but the intensities of Cr_2O_3 and Cr_3C_2 appear to be greater on the scuffed than on the burnished portion. Under the microscope, patches of loose-appearing material with the color and texture of red and black iron oxides and giving dissolution reactions for iron were observed in the surface depressions, apparently as left after pickup from the mating steel slider.

The variations in hardness among the different surface conditions are graphically illustrated in figure 8. Crystallite-size determination showed no large differences. A decrease in crystallite size was expected approaching scuff and such a trend was indicated, but the differences were within experimental error. The sizes were of the order of 14×10^{-7} centimeters.

Electron-diffraction examinations of unscuffed chrome-plated rings taken from steel aircraft-engine cylinders produced no usable patterns. Only high background was observed. Under the microscope, the surfaces had the appearance of having a high polish. X-ray diffraction of these surfaces also showed considerable diffuse scatter together with very diffuse and faint lines whose approximate spacings were those of Cr_2O_3. Electrographic analyses identified chrome and iron, and a series of reactions by metallographic reagents strongly indicated the presence of the compound $Cr_2O_3 \cdot FeO$.

Cast-Iron Surfaces

Two cast-iron slider specimens were examined that had been subjected respectively to a normal and to a prolonged run-in procedure. The prolonged run-in increased load-carrying capacity. Figure 7 lists an X-ray diffraction pattern from an unrun surface showing the presence of α-Fe and one weak ring (interplanar spacing, 4.5 A) that coincides with the strongest line of the graphite pattern. A number of weak lines and one strong line coincide with all the strong lines of Fe_3C, and several unidentified lines also show. On all the surfaces, α-Fe was observed. The presence of graphite was more completely indicated on the worn and scuffed surfaces. Hardness values showed decrease as scuff condition was approached (fig. 9) and crystallite sizes increased.

No examinations were made of used unplated cast-iron piston rings; the information presented in references 2 and 3 is considered sufficient for comparison. These references discuss the detection of the presence of graphite and oxides on surfaces that were in sliding contact during engine operation.

Correlation of Results

In general, the results may be divided into three classes: chemical reaction, material hardening, and alteration of crystallite size. The chemical and physical changes identified on surfaces from the reciprocating slider were superficial compared with the changes wrought on surfaces during engine tests. The depths of the changes were as follows:

Specimen	Depth of change (in.)
Reciprocating slider	1×10^{-5} to 1×10^{-4}
Aircraft-engine-cylinder segment	1×10^{-4} to [a] 1×10^{-3}

[a]Except that 1×10^{-4} in. may be maximum for chrome plate.

On all specimens examined, a certain amount of metallic smear and crystal bending was observed on or just under the surface.

The compounds present on engine-cylinder-barrel surfaces were present also on the slider surfaces of the same material. The only differences in the findings were that the various chemical compounds and phases were more easily identified on the slider specimens, and the the cylinder-barrel surfaces definitely showed carbon and the Beilby layer. The diffraction patterns from the surface material on engine specimens often tended to be diffuse.

The strength of the Fe_3O_4 diffraction pattern from the scuff-recovered steel and the strong evidence of the Fe_3C from the scuffed steel indicated that Fe_3O_4 can be associated with scuff resistance and that Fe_3C can be associated with scuff. Caution should be used, however, in basing such a comparison on the evidence in this investigation alone. Evidence for the association of different oxides with different surface conditions may be found in references 4 and 5. A specially prepared Fe_3O_4 surface was found to have excellent properties partly, at least, because it allowed rapid surface-profile break-in without subsequent high wear or scuffing. This oxide was desirable for an extremely fine and granular structure firmly rooted to the base material. It was not too tenacious to resist abrasion and broke down into a very fine polishing medium during rubbing (reference 4). Whenever in the preparation of the oxide surface the red Fe_2O_3 formed, unfavorable results were obtained. The red oxide was soft and nonadherent (reference 5).

The reason for this difference in surface-rubbing characteristics of these two oxides is not exactly known. Either oxide may form on a given surface depending upon temperature and pressure relations. The number of Fe_3O_4 nuclei developed in unit volume in unit time is relatively large and the velocity of crystallization is small and this oxide may occur as an impalpable powder. The red Fe_2O_3, however, is always crystalline (reference 6, pp. 740, 741, 776).

The engine specimens represented run-in and wear conditions entirely different from those imposed on slider surfaces. Mixed hot gases, flame, impact loading of portions of the cylinder surface, and high sliding speeds were considerably different from the room atmosphere, simple frictional heat, slow speed, and steady loading of the slider. Yet both the engine and slider surfaces exhibited the same kinds of change. The long period of operation of the engine, however, affected the depth to which oxygen penetrated.

The occurrence of oxidation in depth only in regions of surface rubbing suggests the occurrence of minute or microscopic voids as faults (or cracks) within the atomic structure or as intergranular voids. (See references 7 to 10.) The density of an uncast metal during working decreases (references 11 and 12), possibly as a result of the propagation of structural faults or the formation of internal voids. Such a decrease should favor penetration and diffusion of other elements, particularly gaseous ones, into the metal. Such relatively deep oxygen penetration is less in agreement with the usual concentration formula, which limits the thickness of an oxide film, than with an activity-gradient formula (reference 13).

The wear profile of engine cylinders showed a depression, or highest wear, at the top of compression-ring travel. In this region of high wear where less oxygen penetration seemed to have occurred, the surface had been worn away almost as fast as the penetration progressed. Farther down the length of the cylinder barrel the rate of oxygen penetration seemed to exceed the rate of wear. As a result, oxides formed within a relatively pliable matrix of steel and possibly gave rise to a desirable surface, combining pliability with decreased abrasion, which was continually renewed under the slow abrasion of operating wear.

Breakdown of lubricant under excessive conditions may account for an amount of carbon sufficient for formation of the carbides. The formation of a carbide-rich phase and the increased surface hardness on boundary-lubricated steel against cast iron is indicated in reference 14.

The crystallite size and the hardness of the wearing surfaces are possibly as important as the chemical reactions. The relations between crystallite size and hardness for steel, chrome, and cast iron vary as shown in figures 4 and 9 and are somewhat complex. The average hardness of the SAE 4140 steel for the scuffed and scuff-recovered surfaces was greater than the average hardness of the unscuffed surfaces, and by similar comparison the crystallite size was smaller. In conjunction with these facts, the formation of the iron oxides and carbide on the scuffed surfaces is noted. If the change in hardness is to be attributed

to one of the other changes, it seems to follow chemical reaction best. The occurrence of Fe_3O_4 in its greatest quantity coincided with the greatest hardness on the scuff-recovered surface, and a drop in hardness on the scuffed surface coincided with an indicated reduction in the amount of Fe_3O_4. This concept of a general relation of hardness to chemical reaction may or may not be weakened, however, by the occurrence of Fe_3C with the lower hardness of the permanently scuffed surface.

The hardness of the chrome surface increased markedly for the burnished surface condition and corresponded with the formation of Cr_2O_3 and Cr_3C_2. The cast iron softened throughout the runs and the crystallite size increased. The end result at scuff was approximately the same for normal and for prolonged run-in. The prolonged-run-in surface, having the higher load at failure, showed slightly less softening than the normal-run-in surface. The more pronounced crystallite-size increase for the worn-unscuffed surface under prolonged run-in seems incompatible with increased resistance to failure. Chemical changes may account for the reversed trend for this material with respect to the over-all trend associated with the other materials, although such changes were undetectable in this case. Relatively, an opposite trend is indicated for any one of these materials when the change in hardness is compared with change in crystallite size between unscuffed and scuffed surface conditions.

SUMMARY OF RESULTS

The following observations were made as a result of examinations of metallic surfaces that had undergone rubbing under conditions of partly boundary and partly hydrodynamic lubrication; the changes found on steel, chrome, and cast iron varied with the run-in and scuffed surfaces.

The principal chemical reactions were oxidation and carburization with the following reaction products:

Specimen	Surface condition	Material identified on surface	Questionable identification[1]
SAE 4140 steel reciprocating slider	Unrun	α-Fe	Fe_3O_4
	Worn unscuffed	α-Fe	Fe_3O_4, Fe_2O_3
	Scuff recovered	α-Fe, Fe_3O_4	Fe_3C, Fe_2O_3
	Scuffed	α-Fe, Fe_3C, Fe_3O_4	Fe_2O_3
SAE 4140 steel aircraft-engine cylinder barrel	Worn unscuffed (Superficial face)	C (graphite), Beilby layer	Mixed oxides
	(Less than 0.001 in. below surface face)	α-Fe, Fe_3O_4, Fe_2O_3	----------
Chrome-plated cast-iron rider	Worn unscuffed	α-Cr	----------
	Burnished	α-Cr, Cr_2O_3, Cr_3C_2	----------
	Scuffed	α-Cr, Cr_2O_3, Cr_3O_2	----------
Cast-iron reciprocating slider	Unrun	α-Fe	Fe_3C
	Worn	α-Fe	C (graphite)
	Scuffed	α-Fe	C (graphite)

[1] Lines best fit pattern of material listed.

Hardness of materials examined varied with degree of surface condition. The crystallite sizes were in the order of 10^{-7} centemeters. The sizes changed with condition of operation.

Flight Propulsion Research Laboratory,
National Advisory Committee for Aeronautics,
Cleveland, Ohio, April 22, 1947.

REFERENCES

1. Barrett, Charles Sanborn: Structure of Metals. McGraw-Hill Book Co., Inc., 1943, pp. 142-143.

2. Nowick, A. S., and Brockway, L. O.: An Electron-Diffraction Examination of Cast-Iron Piston Rings from Single-Cylinder Aircraft-Engine Tests. NACA ACR No. E4J25, 1945.

3. Nowick, A. S., and Brockway, L. O.: Occurrence of Iron Oxides on Cast-Iron Engine Surfaces after Operation. NACA ACR No. E5L18, 1945.

4. Teetor, Macy O.: The Reduction of Piston-Ring and Cylinder Wear. SAE Jour. (Trans.), vol. 42, no. 4, April 1938, pp. 137-140, 156.

5. Roensch, Max M.: Piston-Ring Coatings and Their Effect on Ring and Bore Wear. SAE Jour. (Trans.), vol. 46, no. 5, May 1940, pp. 221-228.

6. Mellor, J. W.: Ferric Oxide. Ferrosic Oxide; or Magnetic Oxide of Iron. Vol. XIII of A Comprehensive Treatise on Inorganic and Theoretical Chemistry, pt. 2 of Iron, ch. LXVI, sec. 29-30, Longmans, Green and Co., 1954, pp. 731-831.

7. Crussard, C.: Défauts de structure et propriétés mécaniques des métaux. Contribution à l'étude de la structure mosaïque. Métaux. Corrosion - Usure, vol. XX, no. 225-226, May-June 1944, pp. 56-66.

8. Griffith, A. A.: The Phenomena of Rupture and Flow in Solids. Philos. Trans. Roy. Soc. (London), ser. A, vol. 221, March 1921, pp. 163-198.

9. Zener, C., and Holloman, J. H.: Plastic Flow and Rupture of Metals. Am. Soc. Metals. Trans., vol. XXXIII, 1934, pp. 163-215.

10. Bragg, W. L.: The Structure of a Cold-Worked Metal. Proc. Phys. Soc. (London), vol. 52, pt. I, no. 289, Jan. 1940, pp. 105-109.

11. O'Neill, Hugh: The Effect of Cold-Work upon the Density of Crystals of α-Iron. Jour. Iron and Steel Inst., vol. CIX, no. 1, 1924, pp. 93-108; discussion, pp. 109-120; correspondence, pp. 121-128.

12. Goerens, P.: On the Influence of Cold-Working and Annealing on Properties of Iron and Steel. Parts I and II. Jour. Iron and Steel Inst., Carnegie Scholarship Memoirs, vol. III, 1911, pp. 320-434.

13. Darken, L. S.: Diffusion in Metals Accompanied by Phase Change. Tech. Pub. No. 1479, Am. Inst. Min. and Met. Eng., Aug. 1942.

14. Sakmann, B. W.: Metallurgical Transformations in Metal Surfaces under Conditions of Boundary Lubrication. Abs. contributed paper, Am. Phys. Soc. (New York), Jan. 19-20, 1945. Phys. Rev., vol. 67, nos. 5-6, March 1-15, 1945, p. 200.

15. Lipson, H., and Petch, N. G.: The Crystal Structure of Cementite, Fe_3C. Jour. Iron and Steel Inst., vol. CXLII, no. II, 1940, pp. 95P-103P; correspondence, pp. 104P-106P.

BIBLIOGRAPHY

Bowden, F. P., and Hughes, T. P.: The Friction of Clean Metals and the Influence of Absorbed Gases. The Temperature Coefficient of Friction. Proc. Roy. Soc. London, Ser. A, vol. 172, no. 949, Aug. 3, 1939, pp. 263-279.

Bowden, F. P., Moore, A. J. W., and Tabor, D.: The Ploughing and Adhesion of Sliding Metals. Jour. Appl. Phys., vol. 14, no. 2, Feb. 1943, pp. 80-91.

Bowden, F. P., and Tabor, D.: The Theory of Metallic Friction and the Role of Shearing and Ploughing. Bull. No. 145 of Commonwealth of Australia Council for Sci. Ind. Res., Friction and Lubrication Rep. No. 1, Part 1, Melbourne, 1942.

Dies, Kurt: Fretting Corrosion, A Chemical-Mechanical Phenomenon. Eng. Digest, vol. 5, no. 11, Nov. 1944, p. 324. (From V.D.I. Zeitschr., vol. 87, no. 29-30, July 1943, pp. 475-476.)

Finch, G. T.: The Structure of Sliding Surfaces. Engineering, vol. 159, no. 4131, March 16, 1945, p. 215.

Hughes, T. P., and Whittingham, G.: The Influence of Surface Films on the Dry and Lubricated Sliding of Metals. Trans. Faraday Soc., vol. XXXVIII, part 1, no. 249, Jan. 1942, pp. 9-27.

Rosenberg, Samuel J., and Jordon, Louis: The Influence of Oxide Films on the Wear of Steels. A.S.M. Trans., vol. 23, Sept. 1935 pp. 577-598, discussion, pp. 598-613.

Teetor, Macy O.: Load-Carrying-Capacity Phenomena of Bearing Surfaces. S.A.E. Jour. (Trans.), vol. 47, no. 6, Dec. 1940, pp. 497-503.

Webbs, Wells A.: The Influence of Iron Oxide on Wear of Rubbing Surfaces. Sci., vol. 99, no. 2575, May 5, 1944, pp. 369-371.

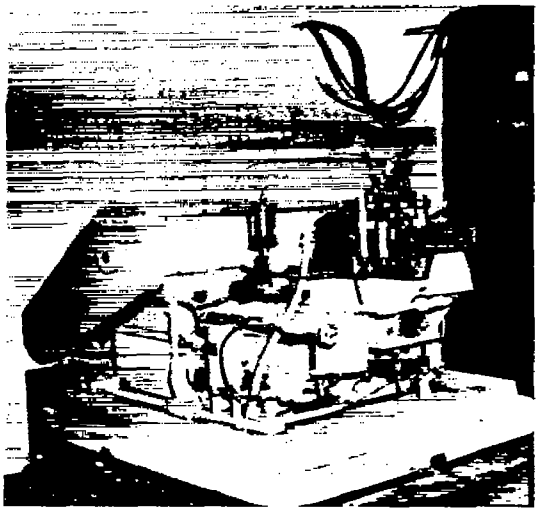

General view

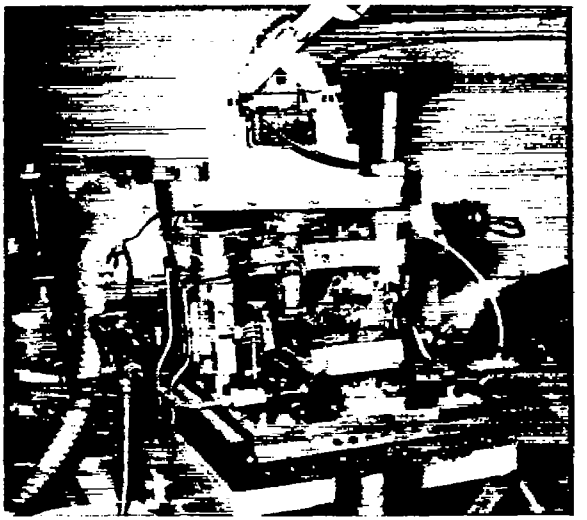

Detail of rider-loading mechanism

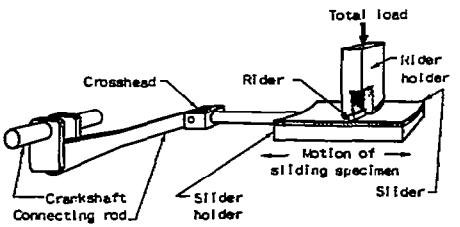

Schematic drawing of elements

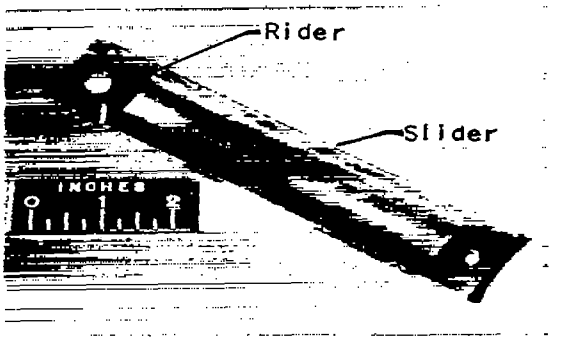

Typical specimens: rider and slider

NACA
C. 16077
10-23-46

Figure 1. - Reciprocating slider machine.

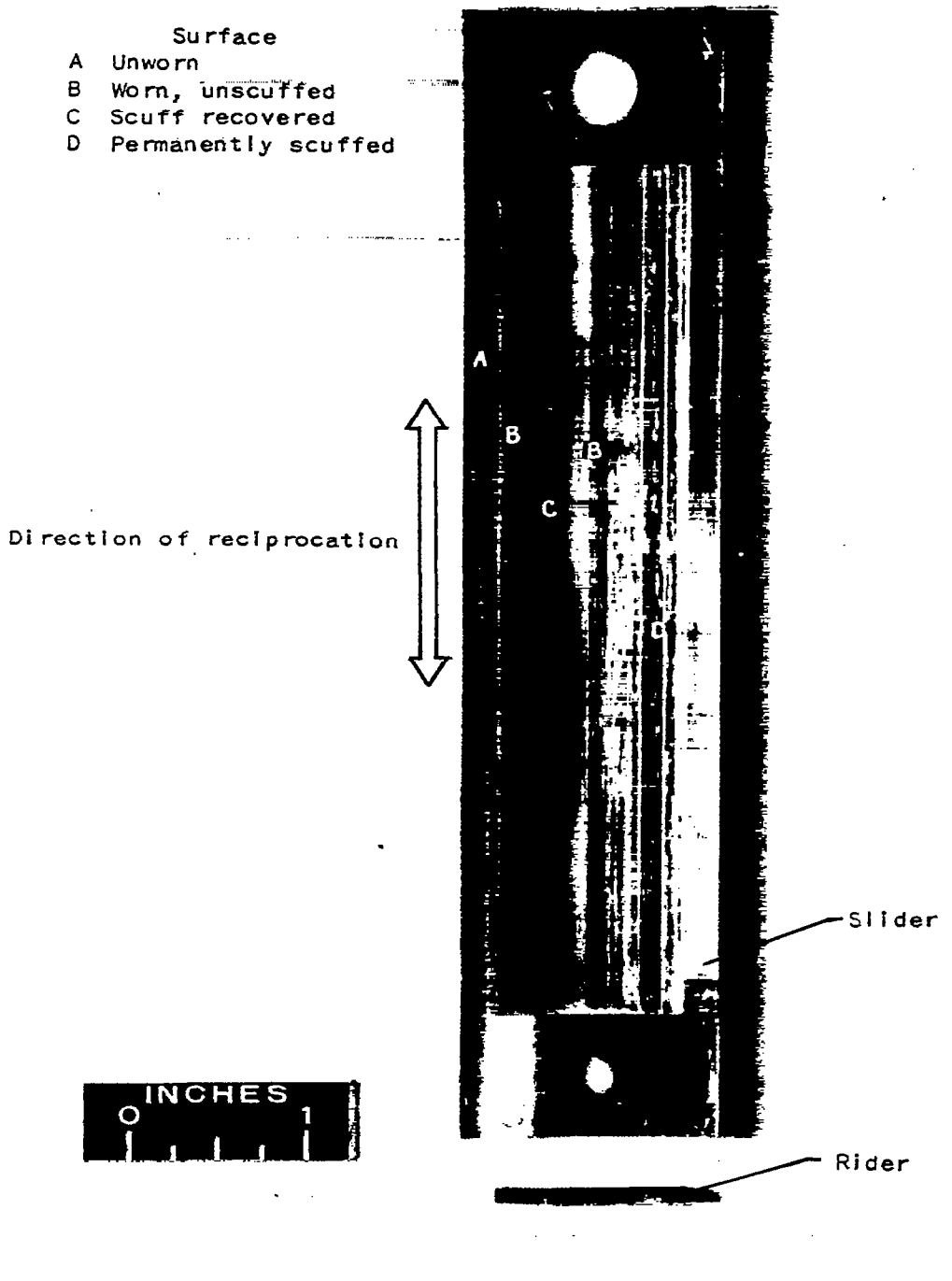

Figure 2. - Run-in and scuffed SAE 4140 steel slider and cast-iron rider showing types of surface on slider.

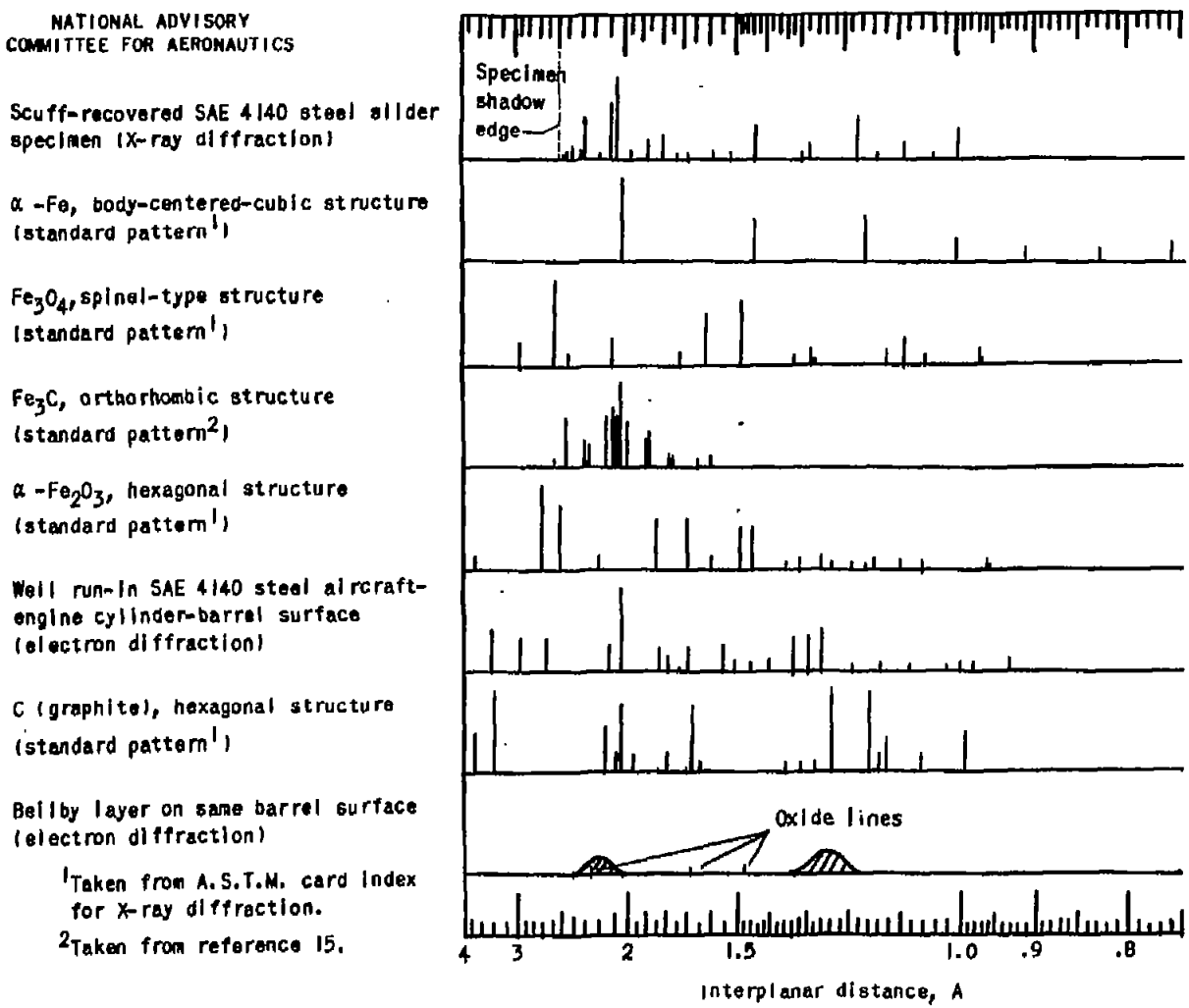

Figure 3. - Typical electron and X-ray diffraction patterns from surfaces of specimens of SAE 4140 steel slider and aircraft-engine cylinder barrel and standard X-ray diffraction patterns of materials identified.

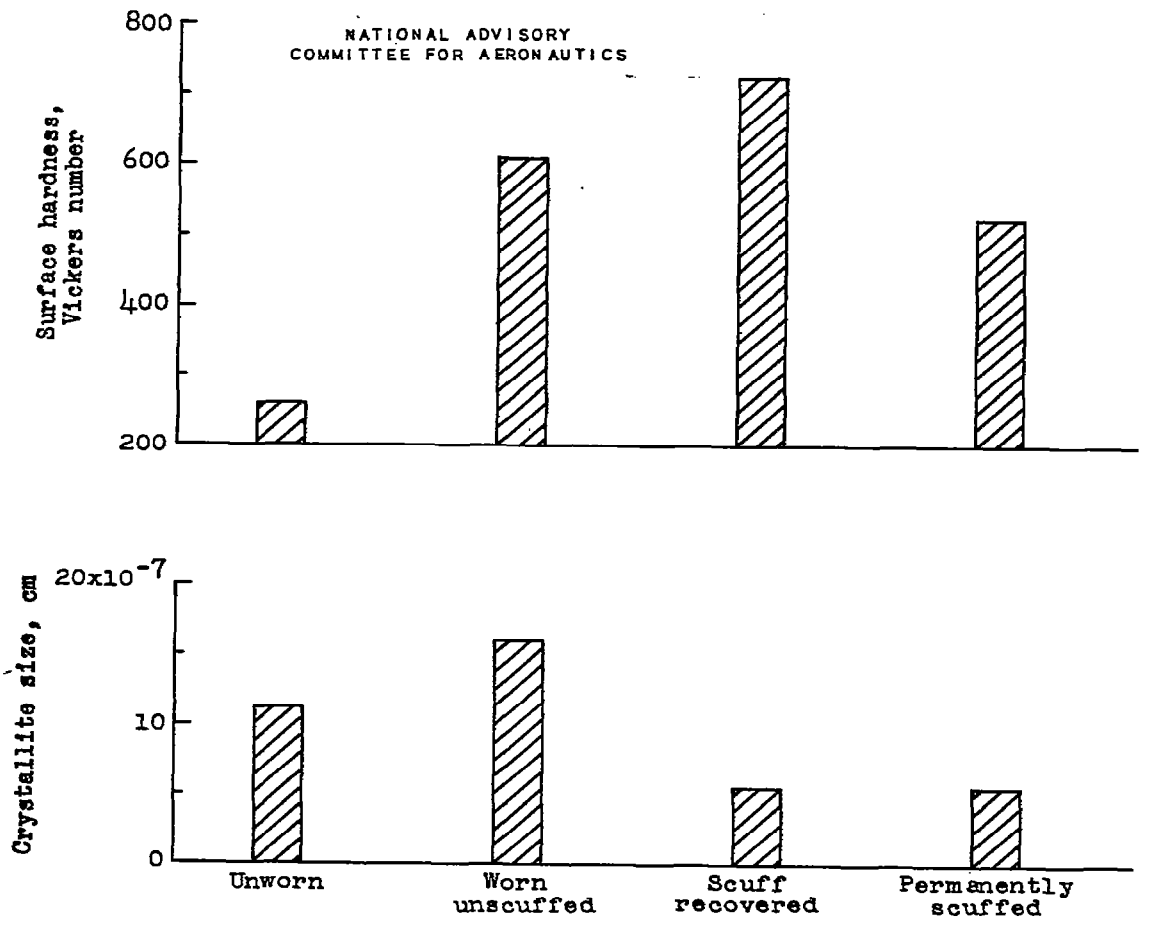

Figure 4. - Relation between surface changes and surface condition of SAE 4140 steel slider specimens.

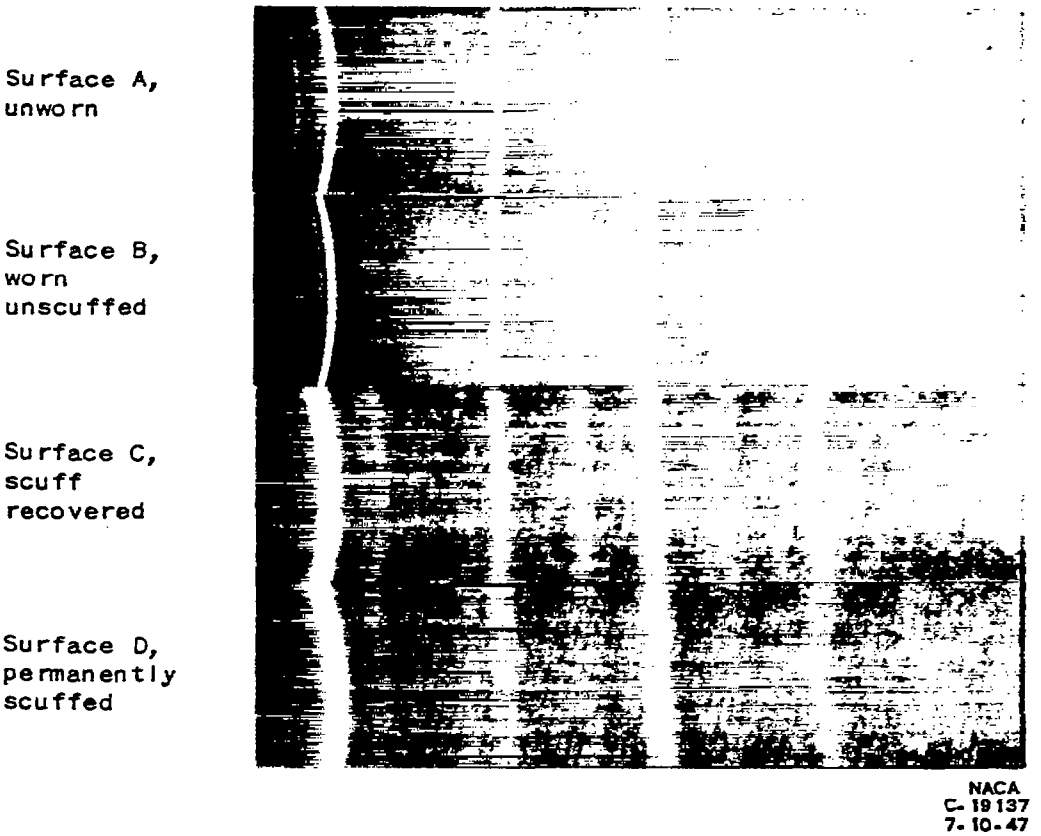

Figure 5. - X-ray diffraction patterns from SAE 4140 steel slider specimen showing change in crystallite size from surfaces A to D.

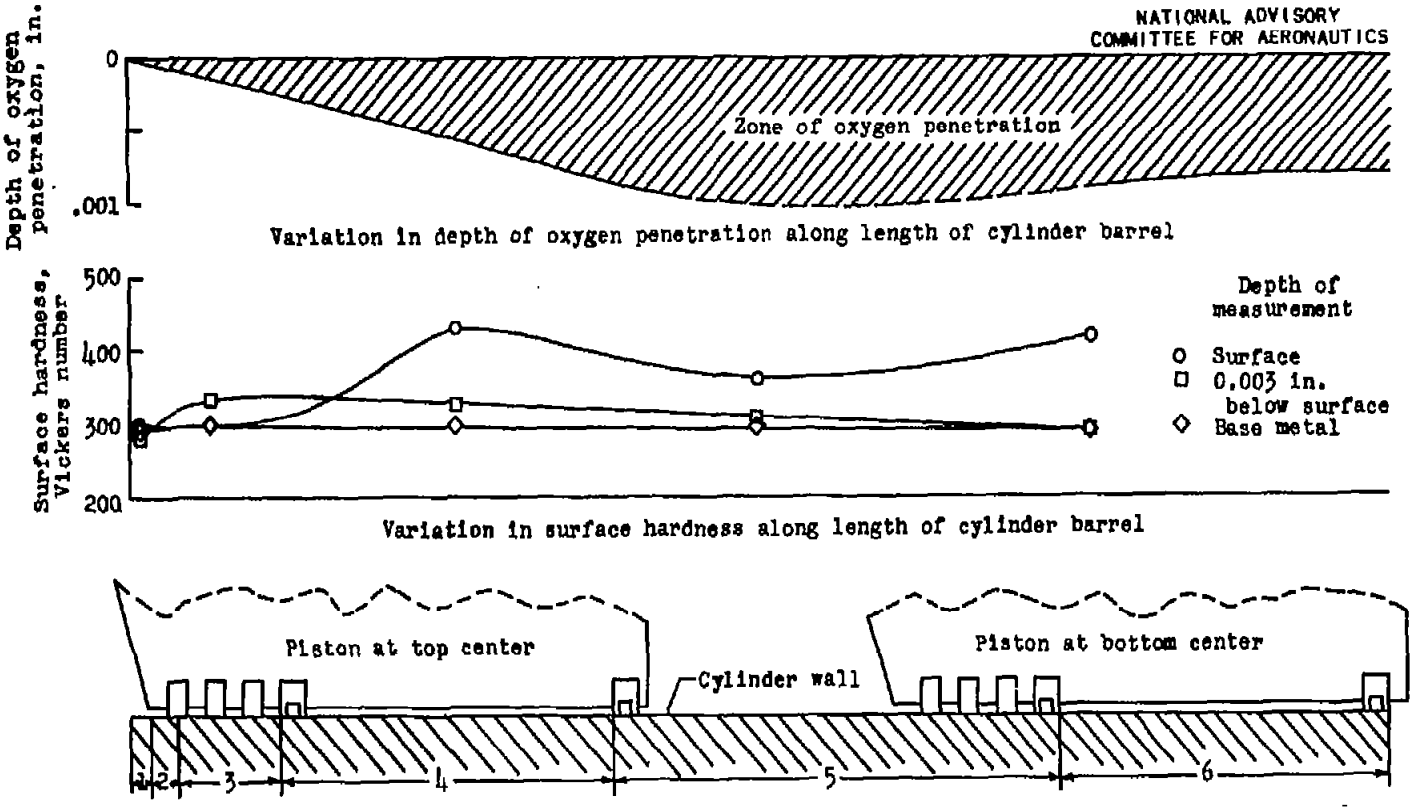

Area number	Location of area on cylinder wall with reference to piston	Piston position	Surface condition
1	Above piston travel	----------	Thin oxide film, no wear
2	Opposite top land	Top center	Light pitting
3	Opposite compression rings	Top center	Heavier pitting and wear
4	Opposite skirt (high sliding speeds)	Top center	Light pitting
5	Opposite compression rings	Bottom center	Low wear
6	Opposite skirt	Bottom center	Very low wear

Figure 6. - Relations among surface condition, material hardness, and depth of oxygen penetration found on worn – unscuffed SAE 4140 steel aircraft-engine cylinder barrel.

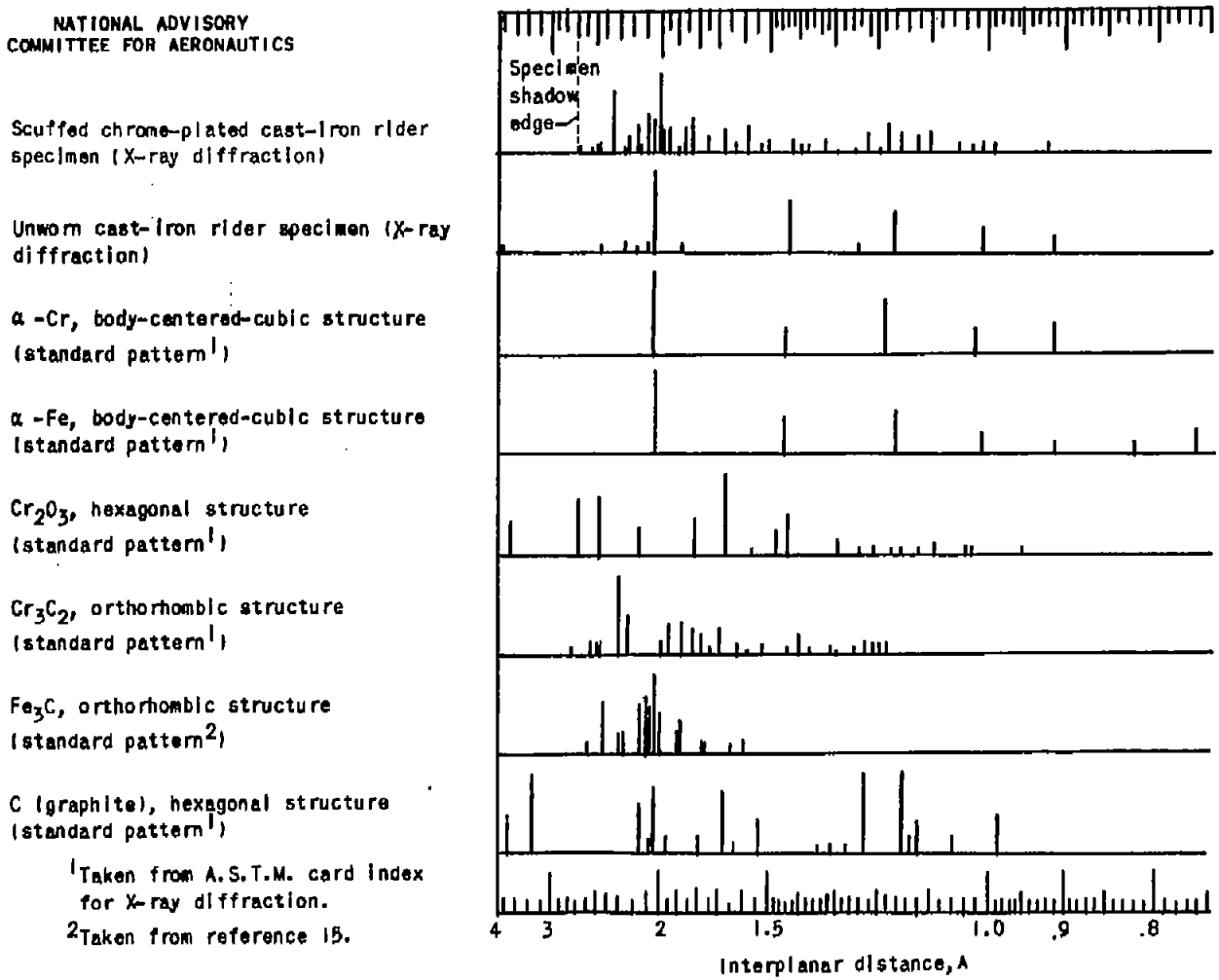

[1]Taken from A.S.T.M. card index for X-ray diffraction.

[2]Taken from reference 15.

Figure 7. - Typical electron and X-ray diffraction patterns from specimens of chrome-plated cast-iron and cast-iron riders and standard X-ray diffraction patterns of materials identified.

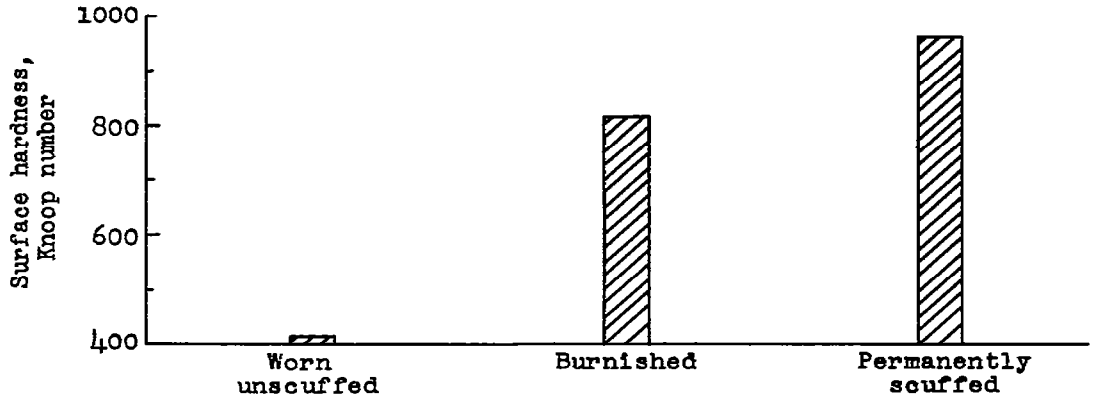

Figure 8. - Relation between hardness and surface condition of chrome-plated cast-iron rider specimen.

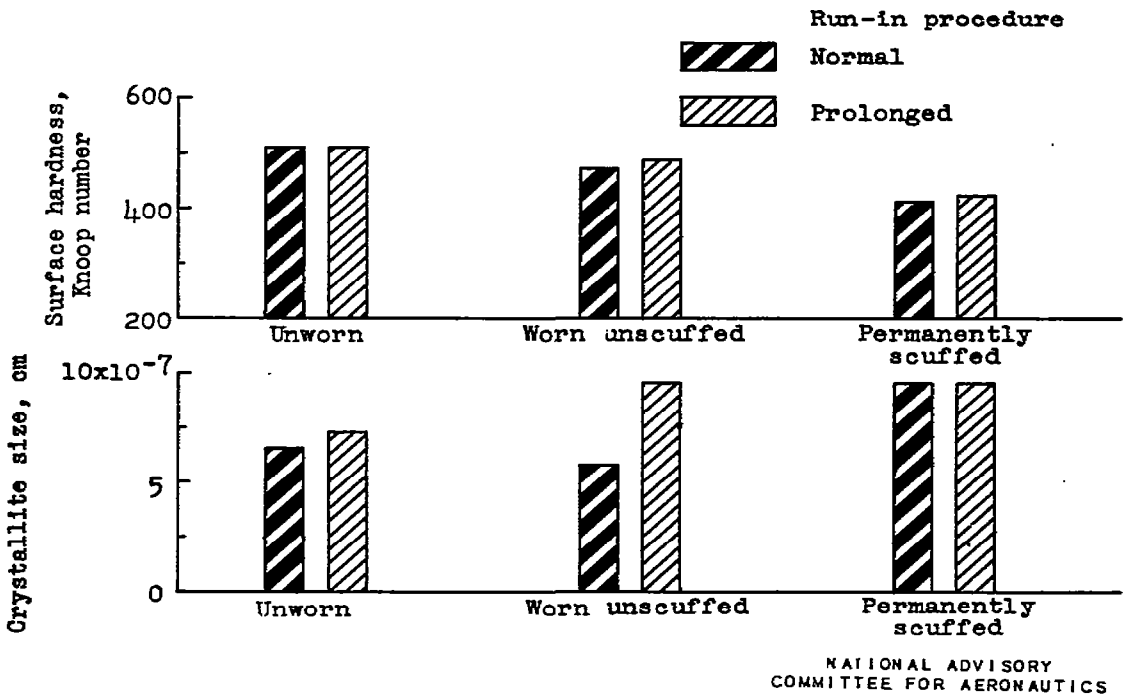

Figure 9. - Relation between surface changes and surface condition of cast-iron slider specimens.